Hydrogen and the magnetic interlayer exchange coupling: Variable magnetic interlayer correlation in Ho/Y(00.1) superlattices

Vincent Leiner,* Murat Ay, and Hartmut Zabel
Institut für Experimentalphysik/Festkörperphysik, Ruhr-Universität Bochum, D-44780 Bochum, Germany
(Received 16 December 2003; published 30 September 2004; publisher error corrected 1 October 2004)

We report on the influence of deuterium on the magnetic properties and the interlayer exchange coupling in superlattices incorporating the magnetic rare earth holmium. By neutron reflectivity and diffraction we investigate the effect of deuterium on the properties Ho/Y(00.1) superlattices. We find that deuterium up-take occurs with strong preference in the yttrium layers. Via magnetic neutron scattering we establish that for this model rare earth system the interlayer coupling can be effectively suppressed through the introduction of deuterium. The gradual loss of the long-range coherence of the magnetic order mediated by the nonmagnetic yttrium layers is discussed in terms of partial interlayer correlation. In a second Ho/Y(00.1) superlattice, composed of ultrathin holmium films, deuterium is an effective agent to vary the total exchange energy of the system and finite size effects on the ordering temperature T_C are observed.

DOI: 10.1103/PhysRevB.70.104429 PACS number(s): 75.70.Cn, 61.12.−q, 68.55.Ln

I. INTRODUCTION

The effect of magnetic interlayer exchange coupling (IEC) was discovered in 1986 in Fe/Cr multilayers[1] and has since been studied in much detail and in many systems. More recently, in 1997, it was found that in ferromagnetic/paramagnetic superlattices the amplitude and the sign of the interlayer exchange coupling can be varied in a continuous way if the nonmagnetic interlayers, which mediate the coupling, dissolve hydrogen. This has been demonstrated for Fe/NbH_x (Ref. 2) as well as for Fe/VH_x (Ref. 3), where a sign reversal of the interlayer coupling constant J' can be achieved for specific hydrogen concentrations. As we will establish in this paper for the Ho/Y(00.1) system, the more complex interlayer exchange coupling in rare earth (RE) superlattices can also be tuned with hydrogen. However, since hydrogen may enter both the magnetic and the nonmagnetic layers, more caution is appropriate for interpreting the results.

It is well known that yttrium and the rare earth metal holmium readily take up hydrogen.[4] In these metals, the introduction of hydrogen leads to the formation of three phases with different crystal structures: (a) the hexagonal α phase at low hydrogen concentrations. In this phase, the hydrogen behaves like a lattice gas, expanding the host lattice without changing its symmetry. Below $\approx$170 K, the hydrogen orders, forming the α' phase while retaining the host metal's hexagonal-close-packed crystal structure. (b) The cubic β phase at the stoichiometric dihydride composition REH_2 with a tetrahedral occupancy of the interstitial sites; and (c) the hexagonal γ phase near to the trihydride REH_3. A coexistence of different phases is observed over rather large concentration regions: in yttrium, for x between 0.2 and 1.8, the α and β phases coexist, and between 2.2 and 1.7, the β and γ phases coexist. Hydrogen in yttrium films has been used for optical switching between the metallic YH_2 and the transparent YH_3 phase signaling a metal-semiconductor transition.[5]

The long-period antiferromagnet holmium exhibits an incommensurate spin helix below the critical temperature, T_C = 131.5 K. (In the literature the critical temperature of a magnetic system with vanishing spontaneous magnetization such as holmium is often called the Néel temperature and denoted by T_N). The spin helix consists of ferromagnetically ordered moments in the hexagonal basal plane and a turn angle α_{Ho} between the magnetization vector from one plane to the next. The reciprocal lattice vector of the spiral $\tau(T)$ and the turn angle are related via $\alpha_{\mathrm{Ho}} = \pi\tau^{\star}$, where $\tau^{\star}$ is given in reciprocal lattice units of the c axis. The helical magnetic structure is preserved throughout the α phase but with increasing H concentration the Néel temperature drops with a rate of $\approx$1 K per atomic percent of hydrogen and the turn-angle slightly decreases.[6] The dihydride phase exhibits a complex antiferromagnetic structure below about 5 K with a reduced magnetic moment,[7] whereas the trihydride phase shows no magnetic order.

Because of the high solubility of yttrium for hydrogen, Ho/Y superlattices offer a model system for investigating potential switchable interlayer coupling in a rare earth system. Also, Ho/Y superlattices have been studied extensively in the past. It has been found that an interlayer exchange coupling between adjacent Ho layers is mediated by the nonmagnetic yttrium, leading to a coherent propagation of the holmium magnetic spiral through the yttrium interlayers.[8] Such interlayer coupling across Y has also been reported for Dy/Y (Ref. 9), Er/Y (Ref. 10), and Gd/Y (Ref. 11). Both a model based on a scalar Ruderman-Kittel-Kasuya-Yosida interaction[12] and the stabilization of a helical spin density wave in the Y conduction electrons[9] have been proposed as coupling mechanisms. From an experimental point of view, Ho/Y superlattices are highly suitable for magnetic neutron scattering studies because the high atomic moment of Ho of $\approx 10\mu_B$ and the incommensurate helical magnetic structure give rise to intense magnetic peaks (τ peaks) at low q values, where q denotes the momentum transfer normal to the superlattice stack. Furthermore, the very good growth properties achieved in sample preparation via molecular beam epitaxy (MBE) are well established.

II. EXPERIMENT

Two superlattices were grown by MBE: a $[Ho_{27}/Y_{17}] \times 30$ superlattice with "thick" holmium films, and a $[Ho_{11}/Y_{23}] \times 30$ superlattice with "thin" holmium layers. The subscripts denote the thicknesses of the holmium films, d_{Ho}, and the yttrium films, d_Y, respectively, expressed in number of atomic planes (ML) per bilayer. The samples were prepared in a standard fashion[13] on $Al_20_3(1120)$ substrates using a Nb/Y buffer system. The superlattices were capped with Y/Nb/Pd to ensure symmetric interfaces for the Ho blocks. The epitaxial relationships are 110 $Al_20_3 \| 110Nb \| 00.1$ Y, Ho. The Pd cap layer serves both as a protection against oxidation and as catalyst for the hydrogen uptake. The rms-roughness, i.e., the interdiffusion region at the Ho/Y interface, is 2–3 ML.

The neutron experiments were carried out using the ADAM reflectometer[14,15] at the Institut Laue-Langevin, Grenoble. Scans were taken with an unpolarized beam of a fixed wavelength, $\lambda = 4.41$ Å. In order to permit an *in-situ* loading of the sample, a close-cycle refrigerator (DISPLEX) was equipped with a sample container, which, in turn, was connected to an outside loading station by a capillary. For experimental reasons that will be discussed below the hydrogen-isotope deuterium was used in the experiment. The deuterium content in the sample was varied by exposing the sample to increasing partial pressures of deuterium for a given time and at room temperature. The deuterium atmosphere was then removed and the sample cooled to 130 K and below. The different loading states of the samples realized in this work are denoted state I–IV. A temperature range of 10–400 K was accessible during the experiment. In the magnetic scattering experiments, specular and off-specular data were collected simultaneously by using a multiwire ^{3}He position-sensitive detector with an active surface of 190×190 mm^2.

III. RESULTS AND DISCUSSION

A. The Ho_{27}/Y_{17} superlattice

1. Neutron reflectivity

Loading Ho/Y superlattices with deuterium (D) instead of hydrogen offers the advantage of adding a positive scattering length. From neutron reflectivity data it is then possible to decide the preferential occupation of deuterium in one of the sublattices. Due to the considerable cross section of deuterium for neutrons, the scattering length density profile in the sample strongly depends on the D concentration within the different layers. In Fig. 1 neutron reflectivity curves for the pristine superlattice (curve A) and the superlattice loaded at three increasing deuterium concentrations are plotted (curves B–D). Several qualitative but important features are immediately noticeable from the data: For the virgin sample, a superlattice peak corresponding to the Ho/Y bilayer period is clearly observable at $q = 0.05$ Å^{-1}. Also seen are rather distinct oscillations in the reflectivity curve which arise from the approximately 400-Å-thick Nb film of the buffer system which shall not interest us here. With increasing deuterium pressure the superlattice peak first vanishes (curve B), then reappears at further elevated deuterium contents, as can be seen in curves C and D. (Also, the oscillation from the Nb layer can no longer be clearly discerned. Rather, oscillations of a shorter period are seen which are mainly governed by the Y film of the buffer. This change of contrast arises from the incorporation of deuterium in the layers of the buffer and cap systems.)

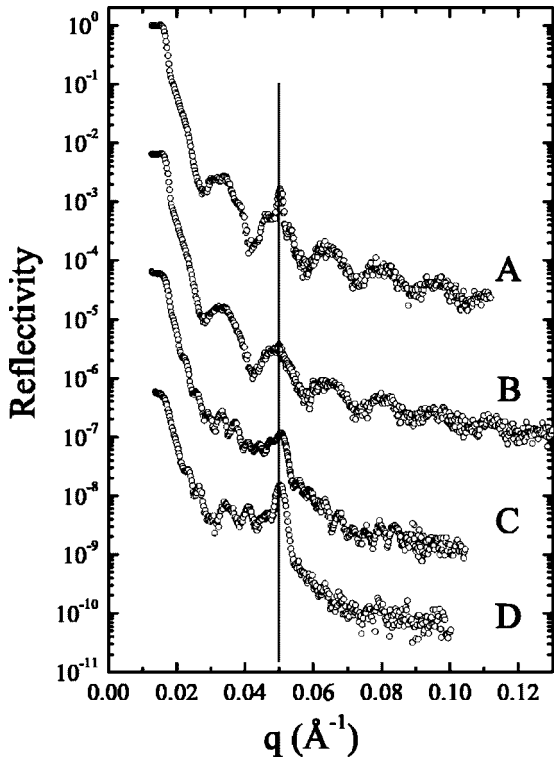

FIG. 1. Specular reflectivity curves taken with an unpolarized neutron beam for different deuterium concentrations. Normalized reflected intensities are plotted vs momentum transfer.

We shall focus on the evolution of the first superlattice peak which monitors contrast changes between the layers that compose the superlattice structure. Table I lists the values for the scattering length densities for yttrium, holmium, and the scattering length b for deuterium. In a neutron reflectivity experiment, the intensity of the first superlattice peak, I_1, is given by

TABLE I. Particle density n, coherent scattering length b and the resulting scattering length density ρ for holmium and yttrium. (All values are bulk values.) Also given is the scattering length of deuterium.

	n (10^{-2} Å^{-3})	b_{coh} (10^{-5} Å)	$\rho = nb_{coh}$ (10^{-6} Å^{-2})
Holmium	3.212	8.01	2.573
Yttrium	3.029	7.75	2.347
Deuterium	⋯	6.67	⋯

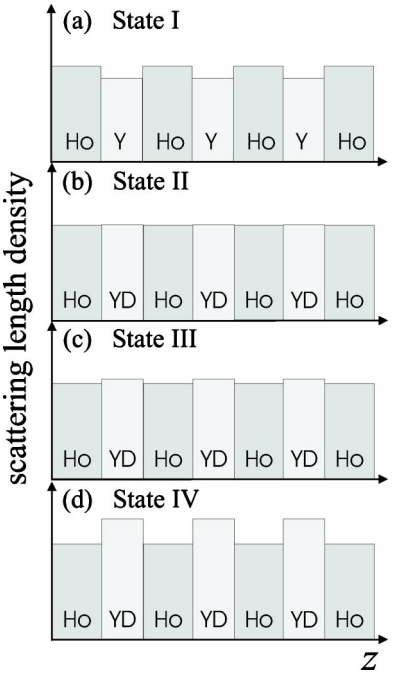

FIG. 2. Representation of the superlattice in terms of the scattering length density. (a) For the pristine sample, contrast arises from the higher scattering length density of holmium (as compared to yttrium), (b) matching of the scattering density after exposure of the sample to deuterium, (c) and (d) contrast is recovered as the scattering length density of the YD_x layers becomes larger than that of holmium. Depicted profiles correspond to the four reflectivity curves shown in Fig. 1, respectively.

$$I_1 \propto |\Delta\rho|^2. \tag{1}$$

$\Delta\rho$ denotes the optical contrast, i.e., the difference in scattering length density between the two materials composing the superlattice structure. In the case of the pristine Ho/Y superlattice (state I, $x=0$):

$$\Delta\rho^I = \rho_{\mathrm{Ho}} - \rho_{\mathrm{Y}} = 0.226 \times 10^{-6}\ \text{Å}^{-2} > 0.$$

In Fig. 2(a) we have given a schematic representation of the profile of the pristine Ho/Y superlattice in terms of the scattering length density. Upon exposure to a deuterium atmosphere, deuterium enters the superlattice and changes the effective scattering length density of the host metal. Returning to the reflectivity data, the loss of contrast observed in curve B can only arise from a matching of the scattering length densities in the Ho and Y layers. Therefore, as the scattering length density of Ho is higher than that of Y (and b_{D} positive), the deuterium uptake has to occur primarily in the yttrium layers. Further we shall make the assumption that the deuterium uptake occurs (almost) exclusively in the yttrium and that only a negligible amount of deuterium enters the magnetic holmium films, as depicted in Fig. 2(b). This assumption is reasonable because of the higher solubility of Y than Ho for deuterium but will also receive further justification later when the magnetic properties of the deuterated Ho/Y superlattices are discussed. In state II, the superlattice peak vanishes and the deuterium concentration x in the yttrium layers can then be estimated from solving the condition for matching scattering length densities

$$\rho_{\mathrm{Ho}} = \rho^{\mathrm{II}} \tag{2}$$

$$b_{\mathrm{Ho}} = \frac{n_{\mathrm{Y}}}{n_{\mathrm{Ho}}}(b_{\mathrm{Y}} + x b_{\mathrm{D}}),$$

where ρ^n denotes the scattering length density of the YD_x layers in state n, and it follows for state II that $x=11$ at. %. It should be noted that using Eq. (2) implies that changes in the lattice constant, i.e., in the particle density n are negligible compared to the deuterium-induced changes of the mean scattering length, $b_{\mathrm{Y}}+xb_{\mathrm{D}}$. That this is indeed the case is seen in Fig. 1 where strong changes in the intensity but not the position of the first superlattice peak are observed. For a similar study of the deuterium profile in a metallic superlattice see, e.g., Ref. 16.

The observed value of x corresponds to the α'-YD_x phase. When the deuterium content in the sample is increased by exposure to an increased deuterium atmosphere, intensity in the superlattice peak—and thus contrast between the Ho and the YD_x films—is recovered. The scattering length density in the YD_x becomes larger than that of Ho, as depicted in Fig. 2(c). For the sample in state III, we can estimate the deuterium concentration by comparing the intensities of the superlattice peak for the pristine sample, I_1^{I}, and the sample in state III, I_1^{III}. From the reflectivity data and using Eq. (1) we obtain

$$\frac{I_1^{\mathrm{I}}}{I_1^{\mathrm{III}}} = \frac{8}{7} = \frac{|\Delta\rho|^2}{|\Delta\rho^{\mathrm{III}}|^2} \tag{3}$$

and with the previously determined value for $\Delta\rho^{\mathrm{I}} = 0.226 \times 10^{-6}\text{Å}^{-2}$:

$$\Delta\rho^{\mathrm{III}} \approx \sqrt{(0.226\ \text{Å}^{-2})^2 \times \tfrac{7}{8}} = 0.211 \times 10^{-6}\ \text{Å}^{-2}. \tag{4}$$

With the *ansatz*

$$\rho_{\mathrm{Ho}} + \Delta\rho^{\mathrm{III}} = \rho_{\mathrm{Y}H_x} \tag{5}$$

the concentration in the yttrium layers of the sample loaded to state III can be evaluated to

$$x = \frac{\dfrac{\rho_{\mathrm{Ho}} + \Delta\rho^{\mathrm{III}}}{n_{\mathrm{Y}}} - b_{\mathrm{Y}}}{b_{\mathrm{D}}} = 22\ \text{at. \%}. \tag{6}$$

Analogously, one obtains for state IV, with

$$\frac{I_1^{\mathrm{I}}}{I_1^{\mathrm{IV}}} = \frac{8}{126} = \frac{|\Delta\rho^{\mathrm{I}}|^2}{|\Delta\rho^{\mathrm{IV}}|^2}, \tag{7}$$

for the difference in the scattering length density

$$\Delta\rho^{\mathrm{IV}} \approx \sqrt{(0.226\ \text{Å}^{-2})^2 \times \tfrac{126}{8}} = 0.9 \times 10^{-6}\ \text{Å}^{-2}, \tag{8}$$

and for the deuterium content in the YD_x layers

$$x = \frac{\dfrac{\rho_{\mathrm{Ho}} + \Delta\rho^{\mathrm{IV}}}{n_{\mathrm{Y}}} - b_{\mathrm{Y}}}{b_{\mathrm{D}}} = 56\ \text{at. \%}. \tag{9}$$

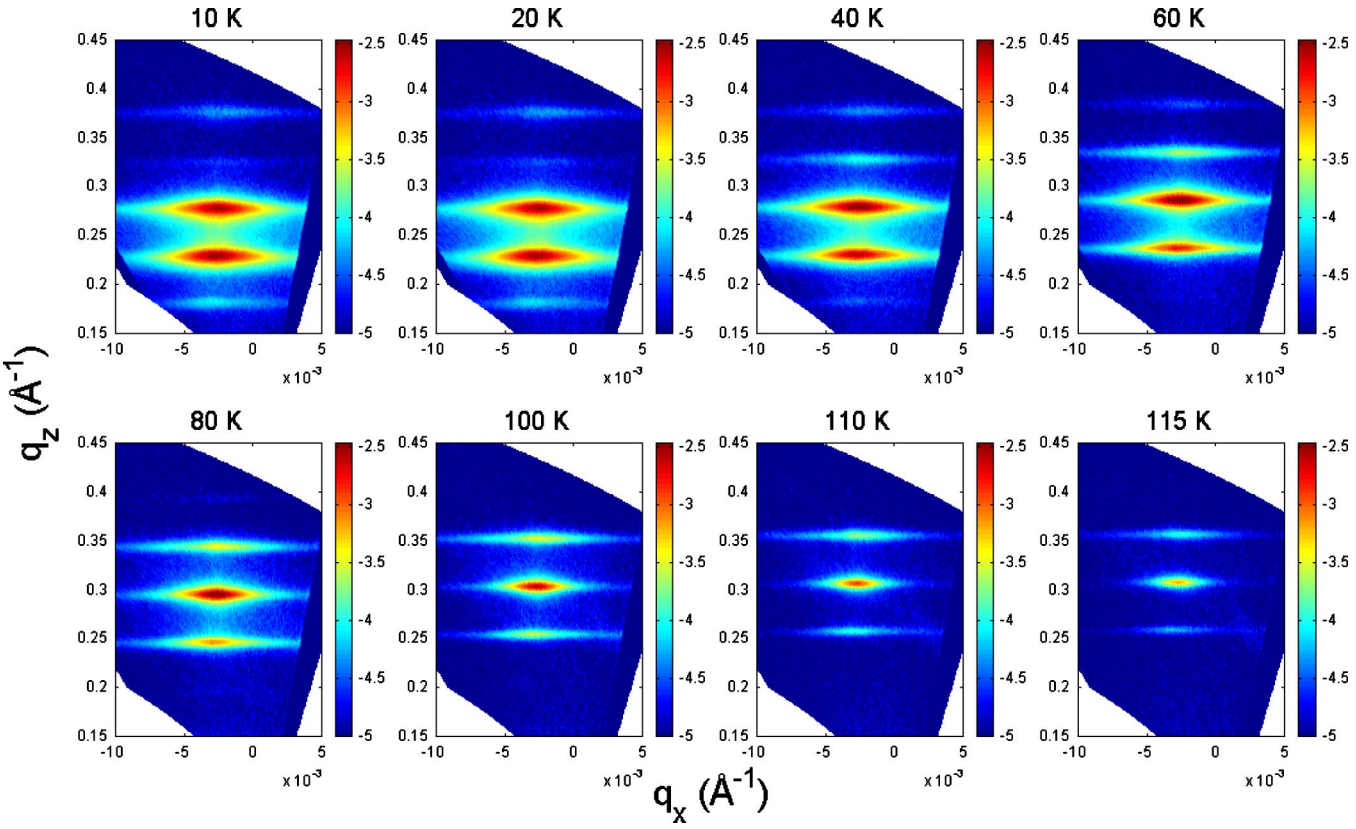

FIG. 3. (Color online) The magnetic (00τ) diffraction peaks of the pristine Ho_{27}/Y_{17} superlattice taken at temperatures between 10 and 115 K. [No intensity was observed in a scan at 120 K. See Fig. 4(a) for spectra taken at 10 and 120 K]. Scattering intensity is plotted as a function of momentum transfer perpendicular and parallel to the sample normal, q_x and q_z, respectively. (The slight shift of the intensity maps in q_x arises from a—frequently observed—tilt of the atomic planes, which are seen in these diffraction patterns, with respect to the physical surface that is seen in a reflectivity experiment. Therefore, an alignment that was perfect for the curves shown in Fig. 1 leads to a small shift here.)

Returning to the reflectivity curves shown in Fig. 1, it can be seen that the introduction of deuterium not only changes the intensity of the superlattice peak but also has a strong influence on the overall shape of the curve. This arises from the rather complicated architecture of the sample: as mentioned earlier, the superlattice was prepared on a Nb/Y buffer system and capped with Y/Nb/Pd. All these layers also take up deuterium so that the scattering length density profile of the entire sample changes with deuterium loading. In our analysis, we focus on the profile of the superlattice stack by investigating the evolution of the first superlattice peak.

In summary, by means of neutron reflectivity measurements, we determined that after exposing Ho/Y(00.1) superlattices to a deuterium atmosphere the deuterium preferentially occupies interstitial sites in the nonmagnetic yttrium layers. This is important as the focus of this work is varying the interlayer coupling mediated by the yttrium layers, rather than the properties of the magnetic holmium films. Also, on the assumption that deuterium is incorporated exclusively in the yttrium layers, an estimate for the deuterium concentration x could be given. This assumption will be further rationalized in the following discussion of the magnetic properties of deuterated (and pristine) Ho/Y(00.1) superlattices.

2. Magnetic neutron scattering

We now turn to the discussion of the magnetic scattering data that were obtained from the pristine superlattice (shown in Fig. 3) and the sample in state IV (shown in Fig. 5).

We recall that in an (elastic) scattering experiment from a crystal the intensity $I(\mathbf{q})$ observed as a function of momentum transfer $\mathbf{q}$ is given by

$$I(\mathbf{q}) = |A_{\text{crystal}}|^2 = \left| \sum_l f(l) e^{i\mathbf{R}_l \cdot \mathbf{q}} \right|^2, \tag{10}$$

where $f(l)$ denotes the scattering amplitude and $\mathbf{R}_l$ the position of lth atom, and the sum is over all atoms of the crystal. In a scattering experiment on thin film systems such as superlattices, the scattering problem becomes one-dimensional and the scattering amplitude A in Eq. (10) can be expressed as a sum over atomic planes. Because a superlattice is a periodic stack of bilayers with period λ_{SL}, the structure factor can be written as the product of the structure factor of one bilayer, where the sum is over all planes in the bilayer, and the superlattice structure factor, where the sum is over all (coherently scattering) bilayers in the sample:

$$I(q) \propto \left| \underbrace{\left(\sum_{m=1}^{N_{SL}} e^{imq\lambda_{SL}} \right)}_{A_{SL}} \underbrace{\left(\sum_{n=0}^{N_{BL}-1} f(n) e^{iqz_n} \right)}_{A_{BL}} \right|^2 . \tag{11}$$

In a neutron scattering experiment on thin single holmium films[17] the helimagnetic structure gives rise to purely magnetic peaks. As the magnetic moment in the holmium planes is rotated by the turn angle α_{Ho} from one basal plane to the next, an incoming neutron with a random orientation of its spin will interact with a periodically modulated scattering potential. If we regard a single bilayer of the Ho/Y(00.1) superlattice, the scattered intensity I is given by

$$I(q) \propto |A_{BL}|^2 \tag{12}$$

$$\propto \left| \sum_n f_n^{mag} e^{in\alpha_{Ho}} e^{iz_n q} \right|^2, \tag{13}$$

where n sums over all atomic planes in one bilayer and the origin $n=0$ is placed in the center of the Ho film. The quantities f_n^{mag} and z_n denote the magnetic form factor and the position of the nth plane, respectively. The term $e^{in\alpha_{Ho}}$ describes the cyclic modulation of f_n^{mag}. Only for the magnetic layers does the factor f^{mag} take on a finite value, in the nonmagnetic yttrium films f^{mag} is zero.

In the present work, we address the question of how the interlayer exchange coupling mediated by the yttrium films, and thus the magnetic interlayer correlation, is affected by the incorporation of deuterium. To analyze the diffraction spectra we use an analytical expression

$$I(q) \propto |A_{BL}|^2 \frac{1-\kappa^2}{1-2\kappa\cos(q\lambda_{SL})+\kappa^2}, \tag{14}$$

as advocated, e.g., in by Giebultowicz *et al.* in Ref. 18 and discussed in more detail by Kepa *et al.* in Ref. 19, in which the authors examine the interlayer correlation in magnetic semiconductor superlattices. In this analysis, the magnetic layers, in our case the holmium films, are not taken to be in a single-domain state with a completely uniform spin structure. Rather, we assume that each holmium layer consists of a large number of magnetic domains. The degree of correlation between the magnetic structures in two adjacent holmium films can be quantified by the fraction $\mathcal{P}$ of correlated domains in two adjacent layers. For $\mathcal{P}\to 1$, the systems become perfectly correlated, while for $\mathcal{P}<1$ correlation is only partial. For $\mathcal{P}=0$ there is no correlation at all, i.e., no interlayer coupling. The parameter κ in Eq. (14) is the fractional correlation coefficient, defined as $\kappa=2\mathcal{P}-1$. It should be noted that the second term in Eq. (14) is constructed in such a way that perfect correlation, $\kappa\to 1$, represents the limiting case for which all domains are correlated and also the number of planes in the sample is infinite. Due to experimental resolution and the finite thickness of the sample, scattering experiments will always yield values of κ well below 1.

Using an unpolarized neutron beam, we performed temperature-dependent measurements of the magnetic $(00.\tau)$ satellite peaks. The pristine $(x=0)$ sample and the sample with maximum deuterium content were investigated in the temperature range 10–120 K. In Fig. 3 the diffraction spectra measured between 10 and 115 K are plotted as a function of momentum transfer perpendicular, q_z and parallel, q_x, to the sample surface. For a sample temperature of 120 K, no magnetic signal was observed, and we determine from the temperature dependence of the data the temperature at which the magnetic signal vanishes, $T_C=118(2)$ K. Figure 3 shows that the magnetic structure in the pristine sample gives rise to sharp satellite peaks. This is unambiguous evidence that the sample displays (the expected) interlayer coupling and that there is a long-range coherence of the holmium spin structure that is mediated by the yttrium interlayers. For a more quantitative analysis, we turn to the specular diffraction pattern obtained for the sample at 10 K as shown by the open symbols in Fig. 4. The solid line represents a fit to the data points based on the analytical expression Eq. (14) with $|A_{BL}|^2$ calculated according to Eq. (13). From the fit we obtain a Ho turn angle of $\alpha_{Ho}=41°$ and a relative correlation coefficient of $\kappa=0.6$ with $d_{Ho}=27$ ML and $d_Y=17$ ML. In order to demonstrate the effect of a gradual reduction of the fractional correlation, in Fig. 4(b), simulated curves are shown in which κ takes on values between 0.6 and 0. For $\kappa=0$, the case of complete decoupling is realized and the diffraction pattern is given by the structure factor for one bilayer. The

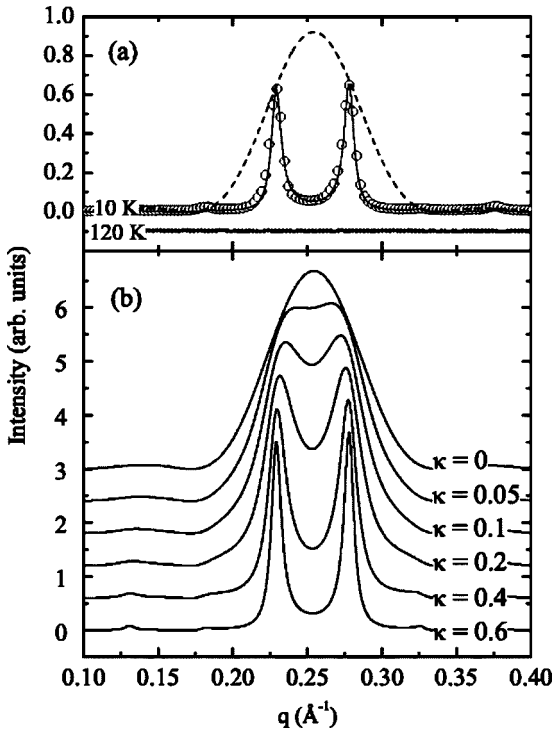

FIG. 4. (a) Specular diffraction pattern at 10 K for the pristine sample (open symbols) and a fit to the data based on Eq. (14) with $\kappa=0.6$ (solid line). The envelop (dashed line) corresponds to the diffraction pattern expected for a stack of uncorrelated Ho films ($\kappa=0$). (b) Spectra calculated for fractional correlation coefficients between 0.6 and 0 to visualize the gradual transition from a highly correlated magnetic structure to a system where interlayer coupling, i.e., correlation, between adjacent Ho films is suppressed.

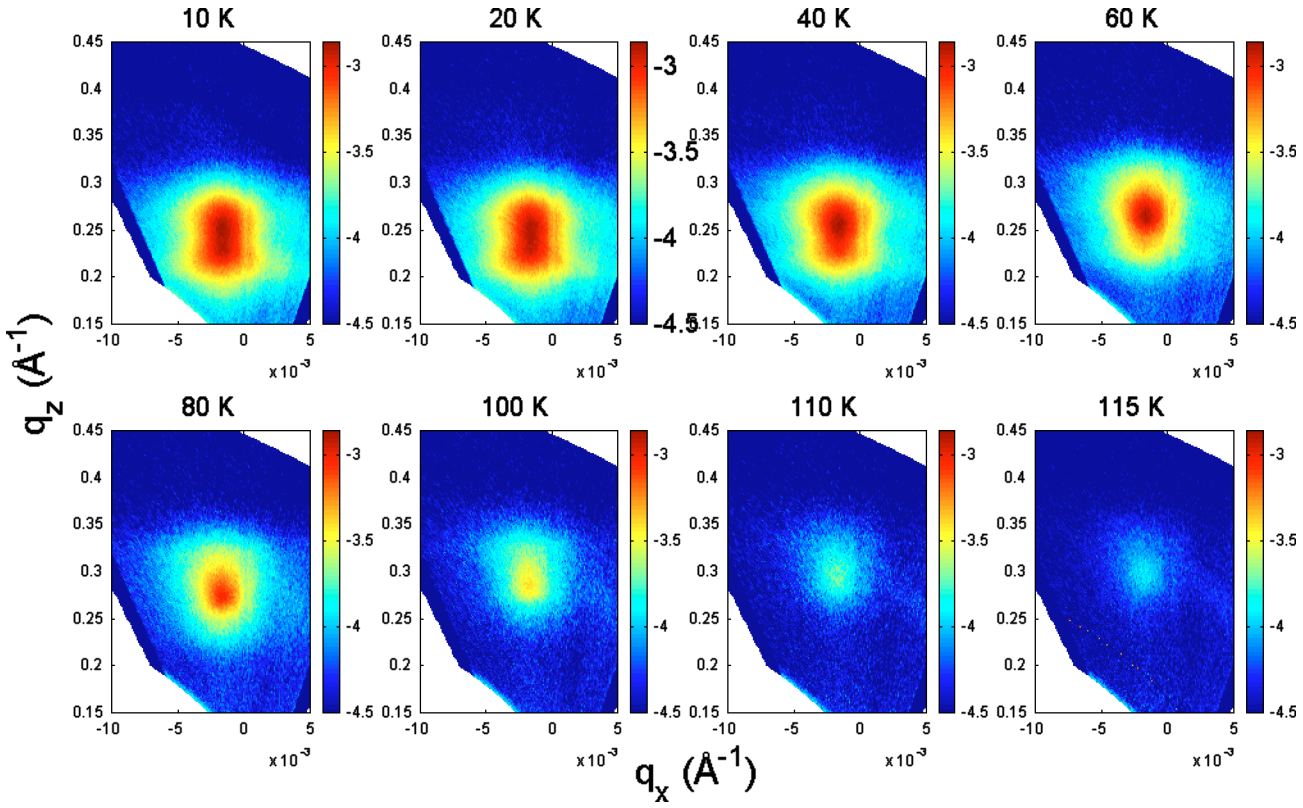

FIG. 5. (Color online) The magnetic (00τ) diffraction peaks of the Ho_{27}/Y_{17} superlattice charged at a deuterium pressure of 60 mbar taken at temperatures between 10 and 115 K. (As for the pristine sample, no intensity was observed in a scan at 120 K.) See also Fig. 6 for line scans extracted from the intensity maps.

$\kappa=0$ curve is also plotted as an envelop (dashed line) in Fig. 4(a).

In the following, we shall turn to the magnetic scattering results obtained from the sample in its final loading stage. In Fig. 5, intensity maps are shown taken at temperatures between 10 and 115 K across the $(00.\tau)$ peak(s). From the data it is evident that upon the introduction of deuterium into the yttrium interlayers the splitting of the τ peak is lost. The broad peak corresponds to the magnetic signal one would obtain from a single isolated Ho film, strongly indicating that the magnetic correlation is lifted by the deuterium uptake in the mediating Y layer. However, the intensity distribution of the loaded sample still exhibits weak features reminiscent of the coupled superlattice, which emerge particularly in the off-specular regime. This means that while a long range propagation of the magnetic helix across the superlattice is suppressed through deuterium uptake, some correlation appears to persist which, however, does not extend over more than a few Ho layers at most. Analogous to the analysis of the magnetic scattering spectrum of the pristine sample, Fig. 6(a) shows the specular scan along the q_z axis extracted from the intensity map for the sample at 10 K. The solid line represents again a fit to the data points of Eq. (14) with $|A_{BL}|^2$ given by Eq. (13). From the fit we obtain a strongly reduced value for the relative correlation coefficient, $\kappa=0.05$, which confirms the earlier notion that the correlation has all but vanished and that deuterium is a suitable agent for varying the interlayer exchange coupling in the rare earth system Ho/Y(00.1). From the temperature dependence of the magnetic signal we find that the deuterated sample display approximately the same ordering temperature as the pristine superlattice, $T_C=118(2)$ K. At the same time we find from the fit to the data that the turn angle has slightly decreased, from $\alpha_{Ho}=41°$ to $\alpha_{Ho}=39.2°$. From the short discussion of the properties of HoH_x films given in the Introduction, we can conclude that some deuterium has entered the Ho films to cause a slight decrease of the turn angle while T_C has remained constant to within 2 K. We can thus estimate a deuterium concentration in the Ho films, $x\leqslant 2$ at. %.

Alternatively, we have simulated the effect of a multidomain state in our sample in which most Ho domains scatter in an independent and uncorrelated fashion, while other domains still show some weak short-range correlation. Figure 7(a) shows a simulated intensity map for independently scattering Ho planes. Because there is no correlation mediated by the yttrium layers, no modulation of the magnetic peak arising from the superlattice structure and thus only a single magnetic peak is observed, at a position given by the turn angle α_{Ho}. The width of the peak in the q_z direction is given by the thickness of the holmium films, d_{Ho}. In the middle panel of Fig. 7, we have simulated the scattering pattern that would be observed from such holmium domains for which some weak correlation persists. (Only the two strongest peaks are seen, while the others vanish into the "background.") In Fig. 7(c), we show the superposition of the two cases shown in panels (a) and (b). The total scattered intensity is given by the incoherent superposition of the scattered intensity from completely decoupled domains and such do-

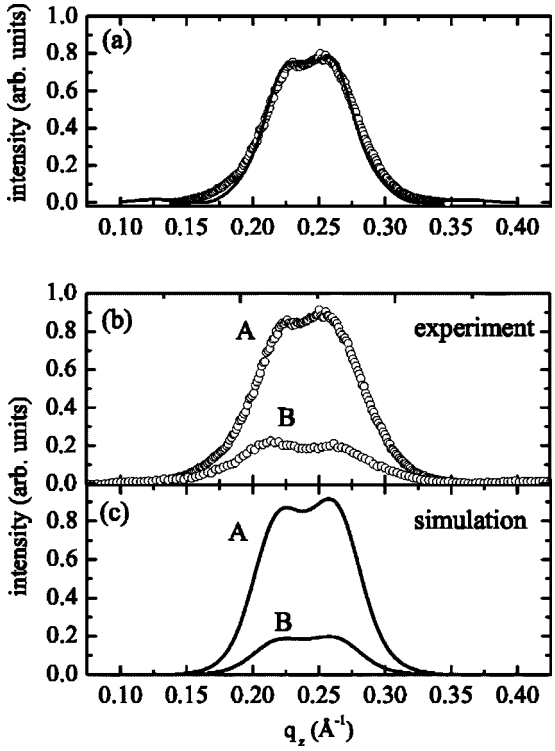

FIG. 6. (a) Specular diffraction pattern at 10 K for the loaded sample (open symbols) and a fit to the data based on Eq. (14) with $\kappa=0.05$ (solid line). (b) Scans along the q_z axis in the region of specular diffraction (curve A) and in the off-specular region (curve B) and corresponding simulated scans extracted as indicated from the simulated map shown in Fig. 7(c).

mains that are still weakly exchange coupled. From the resulting intensity distribution, plotted in Fig. 7(c), we find that the simulation reproduces well the features discerned in the experimental data as shown in the first panel (10 K) of Fig. 3. The very good agreement between simulation and experiment is also evident from Fig. 6(b)–6(c), where we show q_z scans obtained from the experimental intensity map (at 10 K) and the simulation for the specular condition and in the off-specular region (curves A and B).

Summarizing the results from the Ho_{27}/Y_{17} superlattice, by performing temperature-dependent neutron scattering experiments, we have established for the model rare earth system Ho/Y that deuterium is an effective agent for varying the interlayer exchange coupling. We find that by loading the yttrium films into the α-β coexistence region, magnetic interlayer correlation is all but suppressed. A quantitative analysis reveals a fractional correlation coefficient, $\kappa=0.05$, while simulations based on a model of independently scattering domains reproduces well the experimental data both along the specular line and in the off-specular regime.

B. The Ho_{11}/Y_{23} superlattice

For the previously investigated Ho_{27}/Y_{17} superlattice, it was found that, within experimental resolution, the introduction of deuterium into the yttrium spacer layers does not effect the critical temperature at which spontaneous

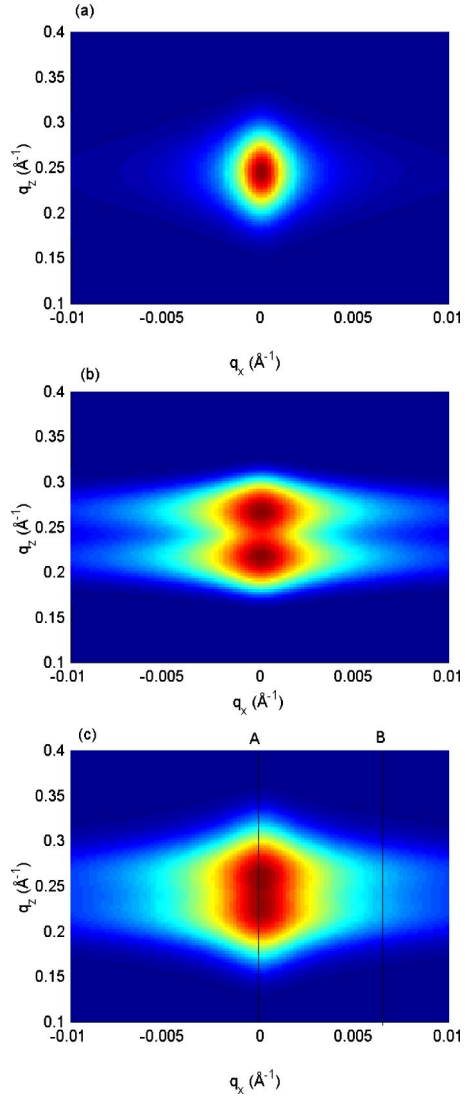

FIG. 7. (Color online) Simulation of the expected intensity distribution at the $(00.\tau)$ position for (a), independently scattering holmium films and (b) for a superlattice in which some short-range correlation across the interlayers is maintained. Bottom panel: incoherent superposition of the patterns shown in panels (a) and (b), representing a multidomain state of the sample.

magnetic order vanishes. For both the pristine and the deuterated sample we observed a constant critical temperature, $T_C=118(2)$ K. From this we were able to deduce that little deuterium is dissolved in the holmium films. In the following we will discuss the magnetic properties of a Ho/Y superlattice with thin holmium films: $[Ho_{11}/Y_{23}]\times 30$. As investigated elsewhere,[20] for thin single holmium metal films, there is a distinct finite-size effect on the magnetic ordering temperatures of such long-period antiferromagnetic structures. We established that the ordering temperature T_C decreases according to the expression

$$\frac{T_C(\infty)-T_C(d_{\mathrm{Ho}})}{T_C(d_{\mathrm{Ho}})}=C_0'\cdot(d_{\mathrm{Ho}}-d_0)^{-\lambda'}, \qquad (15)$$

where $T_C(\infty)$ is the critical temperature for the bulk system, λ' a phenomenological scaling parameter, and C_0 a constant.

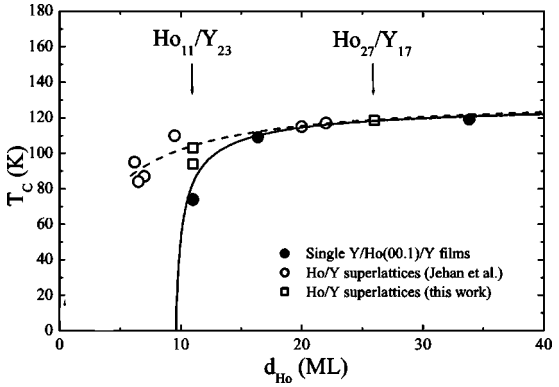

FIG. 8. Finite-size scaling of the critical temperature in holmium single films (solid circles, Ref. 20). Critical temperatures for exchange-coupled Ho/Y superlattices with yttrium interlayers of varying thickness (open symbols, this work and Ref. 8). See text for details.

The finite-size scaling of T_C is shown in Fig. 8 where the critical temperatures observed for a series of single holmium films (solid symbols, Ref. 20) and for several Ho/Y(00.1) superlattices with varying thickness of the yttrium interlayers (open symbols, this work and Ref. 8) are plotted. The solid line reproduces the scaling law as given by Eq. (15).

In Fig. 8, it can be seen that for thicker holmium films ($d_{\mathrm{Ho}} > 16$ ML), the critical temperatures observed for both exchange-coupled Ho/Y(00.1) superlattices and single thin holmium films are primarily determined by d_{Ho}. For $d_{\mathrm{Ho}} \leqslant 16$ ML, it can be seen that the values for T_C, reported in the literature and measured in this work, for a series of superlattices seem to show a considerable scatter and are elevated compared to the T_C value of the single film. This is due to the fact that, for superlattices with very thin holmium films, the contribution of the interlayer exchange coupling to the total exchange energy of the magnetic layers is no longer small. Consequently, the strength of the IEC mediated by the yttrium films strongly influences the experimentally observed critical ordering temperature.

In this context, we have investigated a $[\mathrm{Ho}_{11}/\mathrm{Y}_{23}] \times 30$ superlattice in which a weakening of the interlayer exchange coupling through the introduction of deuterium in the yttrium films and the concomitant loss of interlayer correlation should lead to a reduction of the total exchange energy and thus to a reduction of the critical temperature T_C of the system. Figure 9 shows specular diffraction patterns taken for the pristine sample and with two different deuterium concentrations in the yttrium interlayers. The observed spectra resemble those obtained from the superlattice with $d_{\mathrm{Ho}} = 27$ ML. Due to the reduced thickness of the holmium films we see an increase in the width of the envelop [plotted as a dashed line in Fig. 9(a)]. The diffraction pattern (taken at 10 K) shows again the sharp peaks of an exchange coupled superlattice, and a fit to the data yields a partial correlation coefficient, $\kappa = 0.6$. Through exposure to hydrogen at two different pressures, we realized two successive loading states for the yttrium films, and the corresponding diffraction patterns are shown in the center and bottom panels of the figure. Loss of magnetic interlayer correlation is again observed,

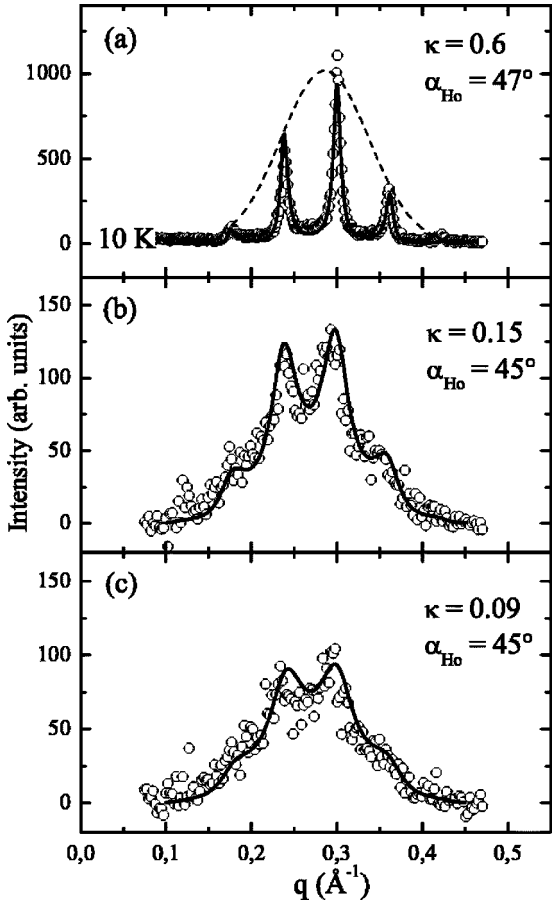

FIG. 9. Specular diffraction pattern of the thin Ho/Y superlattice with (a) no deuterium in the yttrium layers, and (b) and (c), increasing deuterium content. All curves taken at 10 K.

and, from a fit of Eq. (14) to the data, we obtain κ values of 0.15 and 0.09 for the two sample states, respectively. From temperature-dependent measurements of the magnetic peak(s), we determined values for the critical temperature T_C in the three cases. The result is plotted in Fig. 10 where it is shown that a reduction of T_C from 94(3) K for the pristine

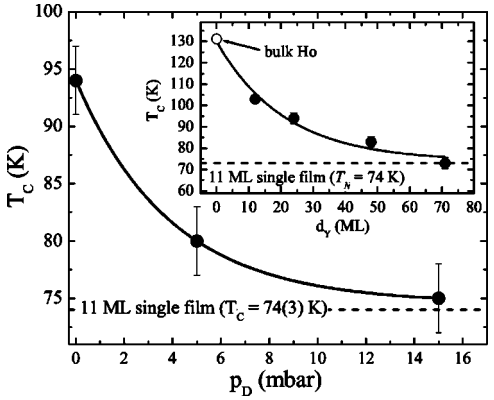

FIG. 10. Critical temperatures of a $\mathrm{Ho}_{11}/\mathrm{Y}_{23}$ superlattice as a function of deuterium content in the yttrium interlayers. Inset: Critical temperatures observed from a series of $\mathrm{Ho}_{11}/\mathrm{Y}_{d_{\mathrm{Y}}}$ superlattices with d_{Y} varied between 12 and 71 ML.

sample to 77(3) K for the final loading stage occurs. Thus we have demonstrated that deuterium in Ho/Y superlattices can be used to vary the strength of the interlayer coupling and thus the total exchange energy of the system in a continuous fashion. For superlattices incorporating thin holmium films finite-size effects become important and a change of the ordering temperature is associated with the introduced change of the total exchange energy. Another, more "traditional" way to vary the interlayer exchange coupling is to vary the thickness of the nonmagnetic spacer layer d_Y. In the inset in Fig 10, we have reproduced the results of a systematic study of $Ho_{11}/Y_{d_Y}]$ superlattices where d_Y was varied between 12 and 71 ML. It is apparent that the two presented mechanisms for varying the strength of the interlayer coupling, i.e., the introduction of deuterium into the yttrium layers or the increase of the interlayer thickness d_Y, lead to a reduction of T_C towards the value observed for an isolated single holmium film, $T_C=74(3)$ K. The solid lines in the inset are guides to the eye.

IV. SUMMARY

We have demonstrated that the exchange coupling in a Ho_{27}/Y_{17} superlattice can be varied through deuterium uptake in the nonmagnetic yttrium layers. Reflectivity measurements confirm that the deuterium resides primarily in the yttrium spacer layer. In the virgin sample, a long-range coherence of the magnetic helix across the Y spacer layer is found. The measured ordering temperature of 118(2) K and the turn angle of the magnetic spiral correspond to the value expected for an isolated single Ho film of 27 ML. At the highest deuterium content in the yttrium layers investigated here an almost complete suppression of the Ho exchange coupling via the Y spacer layers could be observed. Some weak and short-range correlation remained as quantified in terms of a partial correlation coefficient. In Ho/Y superlattice with $d_{Ho}<16$ ML finite-size effects become important and the introduction of deuterium into the nonmagnetic interlayers can be used to vary the total exchange energy of the system in such a way as to strongly influence the ordering temperature of the system, T_C.

ACKNOWLEDGMENTS

Financial support by the German Bundesministerium für Bildung und Forschung through Grant No. 03-ZAE8BO (ADAM project) and the Deutsche Forschungsgemeinschaft through SFB 491 is gratefully acknowledged. The authors are also grateful to D. Labergerie, T. Schmitte, and K. Theis-Bröhl for their support and to A. Remhof for fruitful discussions.

*Present address: Institut für Werkstoffforschung, GKSS Forschungszentrum Geesthacht GmbH, Max-Planck-Str. 1, 21502 Geesthacht, Germany. Electronic address: vincent.leiner@simeonics.com

[1] P. Grünberg, R. Schreiber, Y. Pang, M. B. Brodsky, and H. Sowers, Phys. Rev. Lett. **57**, 2442 (1986).

[2] F. Klose, C. Rehm, D. Nagengast, H. Maletta, and A. Weidinger, Phys. Rev. Lett. **78**, 1150 (1997).

[3] B. Hjörvarsson, J. A. Dura, P. Isberg, T. U. Watanabe, T. J. Udovic, G. Andersson, and C. F. Majkrzak, Phys. Rev. Lett. **79**, 901 (1997).

[4] P. Vajda, *Handbook on the Physics and Chemistry of Rare Earths* (Elsevier Science, New York, 1995), Vol. 20.

[5] J. N. Huiberts, R. Griessen, J. H. Rector, R. J. Wijngarten, J. P. Dekker, D. G. de Groot, and N. J. Koeman, Nature (London) **380**, 231 (1996).

[6] Ch. Sutter, D. Labergerie, A. Remhof, and H. Zabel, Europhys. Lett. **53**, 257 (2001).

[7] E. Grier, Ph.D. thesis, Wolfson College/Oxford University, 2001.

[8] D. A. Jehan, D. F. McMorrow, R. A. Cowley, R. C. C. Ward, M. R. Wells, N. Hagmann, and K. N. Claussen, Phys. Rev. B **48**, 5594 (1993).

[9] R. W. Erwin, J. J. Rhyne, M. B. Salamon, J. Borchers, S. Sinha, R. R. Du, J. E. Cunningham, and C. P. Flynn, Phys. Rev. B **35**, 6808 (1987).

[10] J. A. Borchers, M. B. Salamon, R. W. Erwin, J. J. Rhyne, R. R. Du, and C. P. Flynn, Phys. Rev. B **43**, 3123 (1991).

[11] C. F. Majkrzak, J. W. Cable, J. Kwo, M. Hong, D. B. McWhan, Y. Yafet, J. V. Waszczak, and C. Vettier, Phys. Rev. Lett. **56**, 2700 (1986).

[12] Y. Yafet, J. Appl. Phys. **32**, 48 (1987).

[13] C. F. Majkrzak, J. Kwo, M. Hong, Y. Yafet, D. Gibbs, C. L. Chien, and J. Bohr, Adv. Phys. **40**, 99 (1991).

[14] A. Schreyer, R. Siebrecht, U. English, U. Pietsch, and H. Zabel, Physica B **248**, 349 (1998).

[15] R. Siebrecht, A. Schreyer, U. English, U. Pietsch, and H. Zabel, Physica B **241–243**, 169 (1998).

[16] V. Leiner, H. Zabel, J. Birch, and B. Hjörvarsson, Phys. Rev. B **66**, 235413 (2002).

[17] V. Leiner, D. Labergerie, R. Siebrecht, C. Sutter, and H. Zabel, Physica B **283**, 167 (2000).

[18] T. M. Giebultowicz, H. Kepa, J. Blinowski, and P. Kacman, Physica E (Amsterdam) **10**, 414 (2001).

[19] H. Kepa, G. Springholz, T. M. Giebultowicz, K. I. Goldman, C. F. Majkrzak, P. Kacman, J. Blinowski, S. Holl, H. Krenn, and G. Bauer, Phys. Rev. B **68**, 024419 (2003).

[20] E.Weschke, H. Ott, E. Schierle, C. Schüβler-Langeheine, D.V. Vyalikh, G. Kaindl, V. Leiner, T. Schmitte, M. Ay, H. Zabel, and P. J. Jensen, Phys. Rev. Lett. (to be published).